

Accuracy of Fiber Propagation Evaluation Using Phenomenological Attenuation and Raman Scattering Models in Multiband Optical Networks

Original

Accuracy of Fiber Propagation Evaluation Using Phenomenological Attenuation and Raman Scattering Models in Multiband Optical Networks / Rizzi, G.M., Curri, V.. - In: NETWORK. - ISSN 2673-8732. - ELETTRONICO. - 6:1(2026). [10.3390/network6010016]

Availability:

This version is available at: 11583/3008731 since: 2026-03-13T09:59:00Z

Publisher:

MDPI

Published

DOI:10.3390/network6010016

Terms of use:

This article is made available under terms and conditions as specified in the corresponding bibliographic description in the repository

Publisher copyright

(Article begins on next page)

OPTIMIZATION OF SHELL FE MODELING PARAMETERS IN THE SIMULATION OF WELD FILLETS USING THE STRUCTURAL STRESS METHOD

Leonel Echer

Rogério José Marczak

Mechanical Engineering Department, Federal University of Rio Grande do Sul

Rua Sarmento Leite 425, Porto Alegre, RS 90050-170, Brazil

leonel.echer@ufrgs.br

rato@mecanica.ufrgs.br

Abstract. *The scope of the present work consists of the optimal parameters evaluation for simulating welded structures using shell finite elements. The design variables in the proposed formulation were defined as the weld leg length and thickness of the shell element representing the weld fillet. The main goal of the optimizations was to find a range of thickness/leg length which would not change significantly the first natural frequencies, and still deliver results similar to the ones obtained using a solid model. This kind of model is widely applied to dynamic problems in which the structural stress method (hot-spot approach) is employed for fatigue analysis. Sequential linear programming were performed in T-shaped structures with different structural details (FAT class). The structures of study were represented with constant section, different plate thicknesses and depths. An interior point algorithm was employed in the parametric optimizations performed. Different modeling techniques are suggested for each FAT class tested. A comparison with three well established methodologies presented in standards and the literature is also exposed. The differences in the results are compared for first natural frequencies, total mass and hot spot stress.*

Keywords: *hot spot, structural stress, shell FE, parametric optimization.*

1. INTRODUCTION

The first studies of local stress field on the surroundings of discontinuities as weld toes began in the early 1960's. As presented by Radaj et al. (2006), the local stress field is responsible for crack initiation and propagation. As a result from analysis performed on moderately-thick tubular joints, the structural stress method (hot-spot approach) development occurred during the 1970's (van Wingerde et al., 1995). These analysis showed that the region affected by the local notch, stress peak, extends from $0.3e$ to $0.4e$, where e corresponds to the plate thickness.

Matoba et al. (1983) summarizes the attempts of employing the structural stress method to plate (non-tubular) structures. These attempts took place in the early 1980's and were applied to ship hull details. Radaj (1990) defined the structural stress (σ_{hs}) as the surface stress at the weld toe (hotspot) composed by the summation of membrane (σ_m) and bending (σ_b) stresses. The structural stress was presented as a fictional value with no physical meaning. It was demonstrated that σ_{hs} can be evaluated either by extrapolation or by linearization through the wall thickness. Both procedures has shown to be capable of excluding the stress peak (highly nonlinear) caused by the geometric discontinuity.

After the early 1990's, the structural stress method gained high employability. Various methodologies for representing weld fillets were presented along the decade. Niemi (1994) presented recommendations concerning different approaches for evaluating σ_{hs} , a methodology for modeling the weld fillet using oblique shell elements was proposed as well.

A technique suggesting the use of rigid link elements in order to represent the weld fillet stiffness were presented by Fayard et al. (1997). Based on this methodology, Fermér et al. (1998) proposed a technique using low order shell elements (Volvo method). This technique was initially formulated for thin shell structures and later was extended for structures with moderate plate thickness by Fransson and Pettersson (2000). A methodology for representing the stiffness of the weld fillet without geometrically modeling the fillet was presented by Eriksson and Lignell (2003). It can be accomplished by imposing an increased thickness for the elements in the intersection of different plates, where the weld fillet would exist in the real structure. Dong (2001) proposed two different methodologies (solid and plate/shell elements) based on the structural stress definition presented by Radaj (1990). These techniques are known as the Battelle method. The author claims mesh insensitivity although only simple study cases, most 2D, were presented (Fricke, 2003). It was demonstrated by Niemi and Tonskanen (2000) that these kinds of methodologies fail when representing complex geometries where the transverse shear stress have a greater influence. Measures aiming to circumvent this problem were suggested by Fricke (2003).

Combined effort of different normative entities along with the initiative of the International Institute of Welding, IIW, resulted in a series of recommendations concerning the use of the local approaches for fatigue design of welded components (Hobbacher et al., 2009). This and other recent publications concerning fatigue analysis of welded components, clarified several problems faced when creating finite element models of such structures. The correct selection of extrapolation procedure and distances δ can be easily chosen depending on the weld type. Nevertheless, there is still no consensus about the best methodology for stiffness representation of welded components. This work aims to propose a methodology capable of representing the stiffness of such structures in the most reliable way.

2. STRUCTURAL STRESS METHOD

The structural stress method consists in the evaluation of the surface stress at certain distances from the discontinuity region. Subsequently, these stresses are extrapolated to the weld toe. The structural stress computes the stress increase caused by the structural configuration (macro-geometry). The nonlinear stress peak present on the surroundings of the weld is not enclosed by σ_{hs} (Fricke, 2003), as presented by Fig. 1:

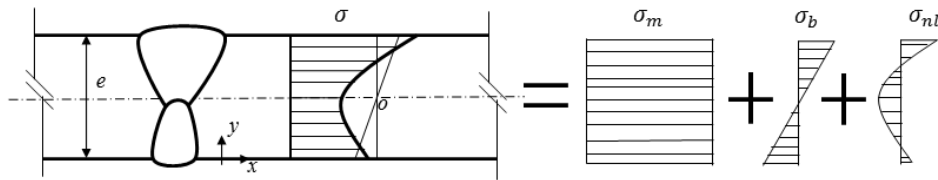


Figure 1. Stress components on the surroundings of a discontinuity [adapted from Hobbacher et al. (2009)].

Once the nonlinear stress, σ_{nl} , component is not taken into account, σ_{hs} can be written as presented by Radaj (1990):

$$\sigma_{hs} = \sigma_m + \sigma_b \quad (1)$$

Figure 2 presents the surface stress in a welded component. The total stress σ shows the influence of the stress peak, while σ_{hs} ignores it. The structural stress is evaluated according to a linear extrapolation performed over the stresses obtained at two reference points. The spacing between the reference points and the weld toe is defined by δ distances. The lengths of δ are defined depending on the refinement of finite element mesh and hotspot type, as presented by Fricke et al. (2001), and Doerk et al. (2003).

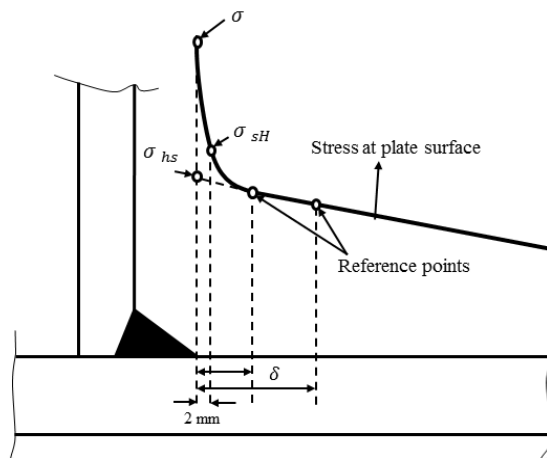


Figure 2. Structural stress extrapolated through δ distances from the weld toe.

3. DIFFERENT MODELING TECHNIQUES

Due to the high computational time required for the simulation of solid models, plate/shell elements are preferred in structural stress analysis. A considerable number of methodologies for weld representation using plate/shell elements were proposed along the last decades by several authors. Nevertheless, there is still no consensus about which one produces the best results for most cases. Moreover, all the existing methodologies for representing welded components using plate/shell FE share a flaw: the stiffness of the real structure is only approximated. In other words, the stiffness of the shell FE model differs from reality, or even from the stiffness of a solid FE model.

Some of the most widely widespread methodologies are discussed below. The methodologies presented were chosen mostly by the fact that their respective authors have provided enough data to permit the reliable reproduction of these methodologies

3.1 Olique shell elements

Niemi (1995) proposed the representation of the weld fillet using oblique shell elements. This is one of the first, and probably the most intuitive, methodologies ever presented. It consists on representing both plates and welds with 8-node shell elements. Figure 3 illustrates this methodology.

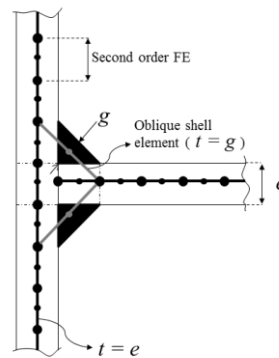


Figure 3. Weld fillet represented by shell oblique elements [adapted from Niemi (1995)].

As illustrated in Fig. 3, the shell element thickness, t , of the elements modeling the weld are equal to the weld throat, g . The rest of the structure is modeled with a shell element thickness equal to the plate thickness, e .

3.2 Rigid link elements

A methodology where rigid links are employed in order to represent the stiffness of the weld was proposed by Fayard et al. (1997). In this technique, σ_{hs} is evaluated directly in the center of gravity, CG, of a shell element. Such element must be positioned to impose the location of its CG in a determined region. This region corresponds to the weld toe occurrence in the real structure. Figure 4 illustrates the methodology presented by Fayard et al. (1997).

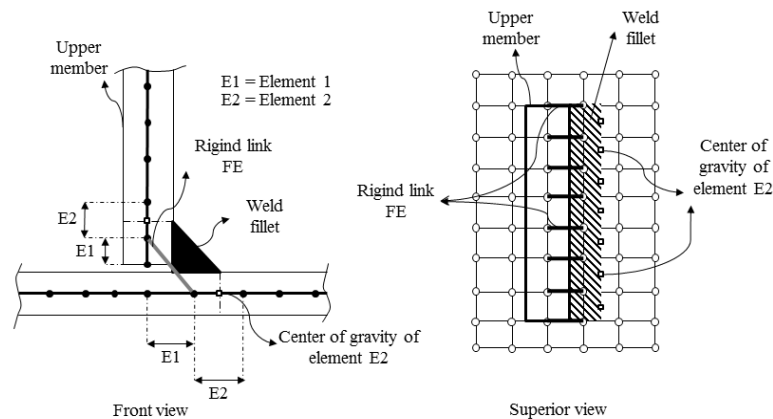


Figure 4. Weld fillet represented by rigid link elements [adapted from Fayard et al. (1997)].

The plates forming the structure must be modeled using 4-node shell elements with the same thickness of the plates. Elements E1 and E2 must have specific sizes, allowing the stress evaluation directly at E2s CG. Such approach discards the use of any extrapolation procedure.

3.3 Increased thickness

Eriksson and Lignell (2003) proposed a modeling technique where the stiffness of the weld is represented without representing the weld fillet. It is afforded by the imposition of an incremented thickness. Such representation demands the physical connection of the plates. Figure 5 represents such methodology applied to a cruciform joint.

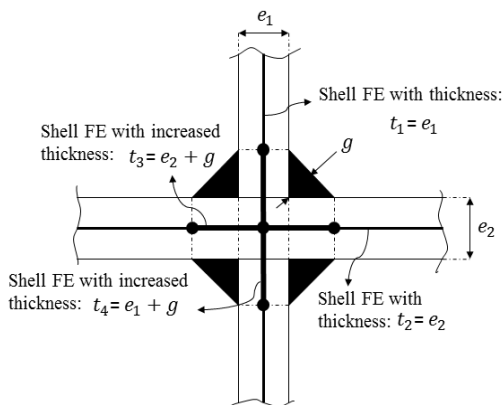


Figure 5. Modeling technique without weld geometrical representation [adapted from Eriksson and Lignell (2003)].

4. PROPOSED METHODOLOGY

As discussed earlier, the presented methodologies, and the majority of the others, share a flaw. Those methodologies only are capable of approaching the weld stiffness. A better modeling technique should be able to reproduce its stiffness in a more reliable way. Unfortunately, a perfect representation is impracticable. However, it is possible to perform a modeling technique where geometrical parameters are chosen in such a way that the error with respect to the weld stiffness could be minimized. A methodology capable of obtaining optimum parameters for modeling welded components is formulated and presented below.

4.1 Geometries of study

The formulated methodology employs the representation of the weld by oblique shell elements as recommended by the IIW (Hobbacher et al., 2009). The parameters chosen to be optimized are the thickness, t , of the FE representing the weld and a distance d . Such distance corresponds to the weld leg length. Two different geometries were chosen to be optimized, the first consist in a T-shaped component with weld fillets without penetration; the second is the same structure, but with weld fillets with full penetration. Respectively, these two geometries correspond to the structural details number 6 and 2 presented by Hobbacher et al. (2009). Figure 6 illustrates these structures and the parameters to be optimized.

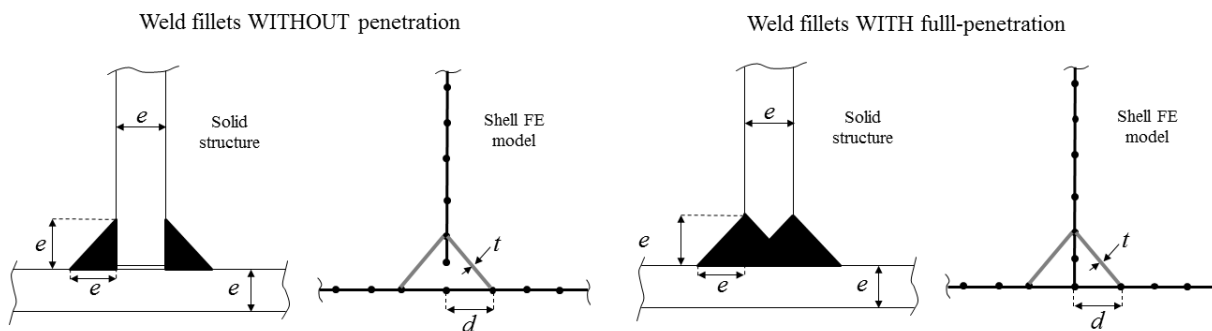


Figure 6. Shell FE representation and parameters chosen to be optimized.

As illustrated, the geometries of study consist on T-shaped joints. The plates forming the joint have the same thickness. Weld fillets are symmetric and have leg lengths equal to the plate's thickness. A generic illustration of the geometries is presented in Fig. 7.

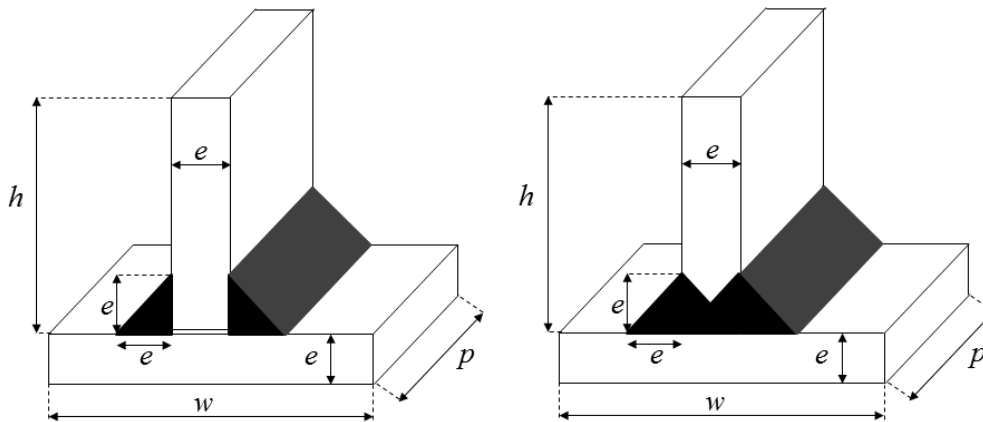


Figure 7. Solid representation of both analyzed geometries.

The height, h , and width, w , are constant for all cases, while the plate's thickness and depths, p , assume different values over the cases. Four different plate thicknesses and 4 different structure depths are employed, totaling 16 cases for each structure. All the geometric parameters considered by the simulations are presented in Table 1:

Table 1. Geometrical parameters of the structure.

Plate thickness:		Height:	Width:	Depth:	
e [mm]	e [inch]	h [mm]	w [mm]	p [mm]	
3.175	1/8	254	254	$2w =$	508
6.35	1/4			$4w =$	1016
12.7	1/2			$6w =$	1524
19.05	3/4			$10w =$	2540

4.2 Parametric optimization formulation

Representations of the structure modeled with solid elements, i.e., idealized T-joint welded components, were employed as reference for the evaluation of the error. The error was evaluated with respect to the structure stiffness. In order to do that, the first natural frequencies of the structure were employed in the Eq. (2). Moreover, the modeling technique was implemented in such a way to conserve the structural mass. In other words, the shell elements representing the weld employed an artificial density, reproducing the same mass of the solid structure. The error function can be written as follows:

$$Err = \sqrt{(\overline{f_1} - f_1)^2 + (\overline{f_2} - f_2)^2} \quad (2)$$

where $\overline{f_i}$ represents the i -th natural frequency of the comparison model, i.e., solid structure idealized representation, and f_i is the i -th natural frequency evaluated with respect to the shell model.

Once the error (objective) function is defined, the constrained optimization problem can be presented according to Eq. (3). The constraint functions with respect to the parameter d are defined considering the physical admissible limits, i.e., plate width w and plate thickness e . While the constraints with respect to t consider as upper limit a shell FE thickness equal to 10 times the plate thickness e , and a lower limit equal to 0.01 times the plate thickness.

$$\begin{aligned}
 & \min_{t,d} \quad Err(f_1, f_2) \\
 & \text{subject to} \quad t_{\max} \leq w/2 \\
 & \quad \quad \quad t_{\min} \geq e/2 \\
 & \quad \quad \quad d_{\max} \leq 10e \\
 & \quad \quad \quad d_{\min} \geq 0.01e
 \end{aligned} \tag{3}$$

All optimizations were implemented in a commercial mathematical software (MATLAB, 2011), and the FE models were solved by a commercial finite element software (ANSYS, 2012). Figure 8 presents an overview of the whole optimization procedure. The stopping criteria employed was a residual error equals or smaller than 10^{-4} . The increment needed by the finite difference method was defined as 10^{-5} . A step length modifier was applied to the actualization of the project variables t and d for each new iteration. Once the new set of parameters was defined by the SLP, the step length was modified according to the two sets of parameters previously defined in past iterations.

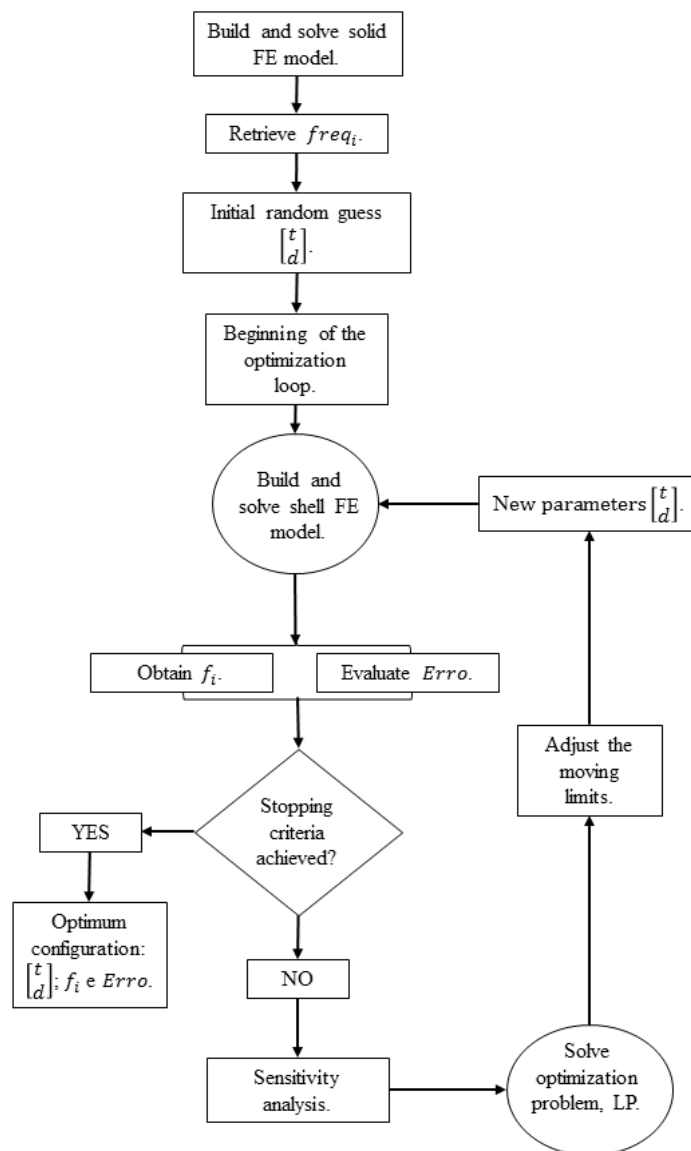


Figure 8. Flowchart for the optimization procedure.

5. RESULTS

The results obtained from the optimization process were employed to formulate a modeling technique for each analyzed geometry, i.e, T-joint without penetration and with full penetration. These modeling methodologies were tested and compared with the three modeling techniques earlier presented in this work. The comparisons were performed with respect to mass error and stiffness error, Eq. (2), the results obtained from a solid model were employed as reference. The two proposed modeling techniques were implemented along the structural stress method in order to evaluate σ_{hs} as well. In order to avoid confusion the initials NP are used to refer to the component with weld fillets without penetration and the initials FP are used to refer to the component with full penetration weld fillets.

5.1 Optimum parameters

Figure 9 present the optimum parameters for different plate thicknesses and structure depths for the geometry with weld fillets without penetration. The agreement between different results clearly evidences a considerable independence of the project variables with respect to the depths p .

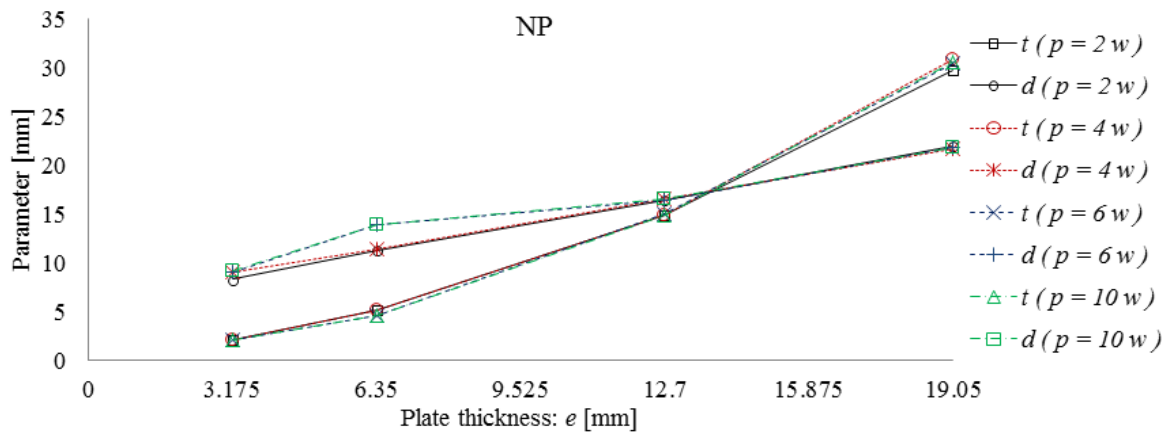


Figure 9. NP – Overlapped optimum parameters.

Once the optimum parameters were evaluated, two different mean values approximation were performed in order to propose a reliable modeling technique. It considers one mean curve for each parameter; trend lines are traced aiming to equate the behavior of t and d with respect to different plate thicknesses e . Figure 10 illustrates Proposal NP:

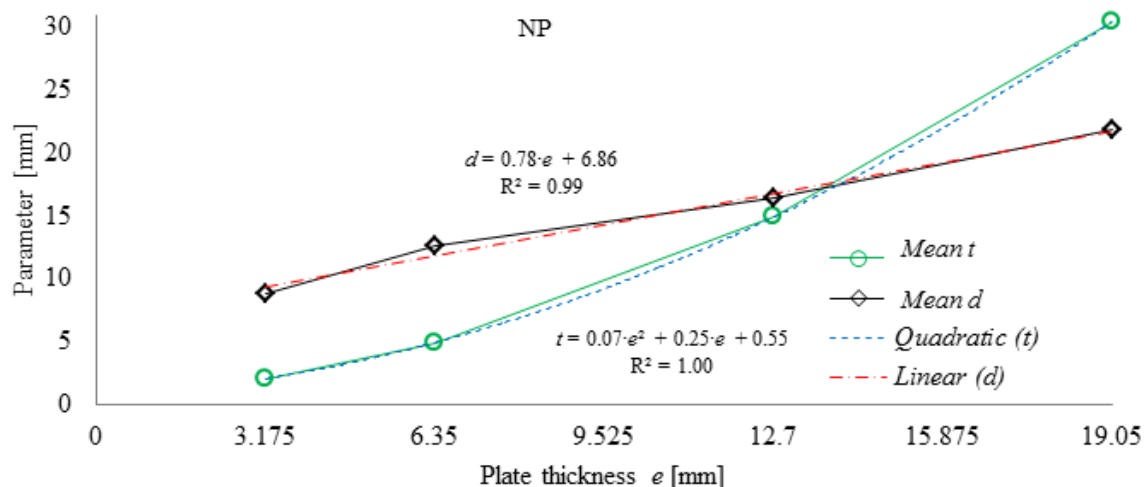


Figure 10. NP – Proposed methodology.

Equations (4) and (5) represent the trend lines employed in Fig. 10. These equations rule the methodology proposed:

$$d = 0.78e + 6.86 \tag{4}$$

$$t = 0.07e^2 + 0.25e + 0.55 \tag{5}$$

Figure 11 presents the optimum parameters for different plate thicknesses and structure depths for the geometry with full penetration weld fillets. Once more, the agreement between different results clearly evidences a considerable independence of the project variables with respect to the depths p .

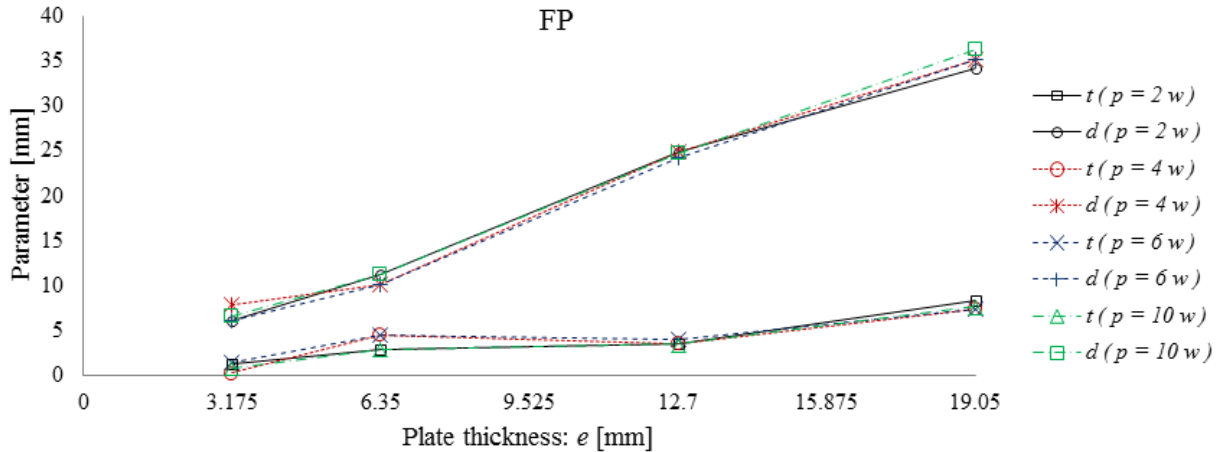


Figure 11. FP – Overlapped optimum parameters.

Analogously, two different mean values approximation were performed and a modeling technique was proposed. It considers one mean curve for each parameter; trend lines are traced in order to equate the behavior of t and d with respect to different plate thicknesses e . Figure 12 illustrates Proposal FP:

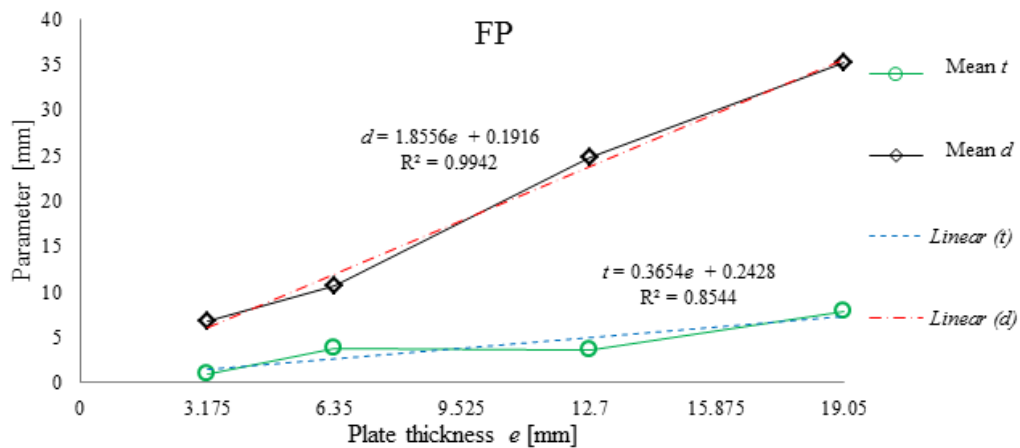


Figure 12. FP – Proposed methodology.

Equations (6) and (7) represent the trend lines employed in Fig. 12. These equations rule the methodology proposed:

$$d = 1.8556e + 0.1916 \tag{6}$$

$$t = 0.3654e + 0.2428 \tag{7}$$

5.2 Comparison of methodologies

The error with respect to the total mass of the modeled structure and the mass of the real structure (solid) is presented in Fig. 13. Both proposed methodologies (Proposals NP and FP) induce the conservation of mass. The other modeling techniques implemented does not count with such feature.

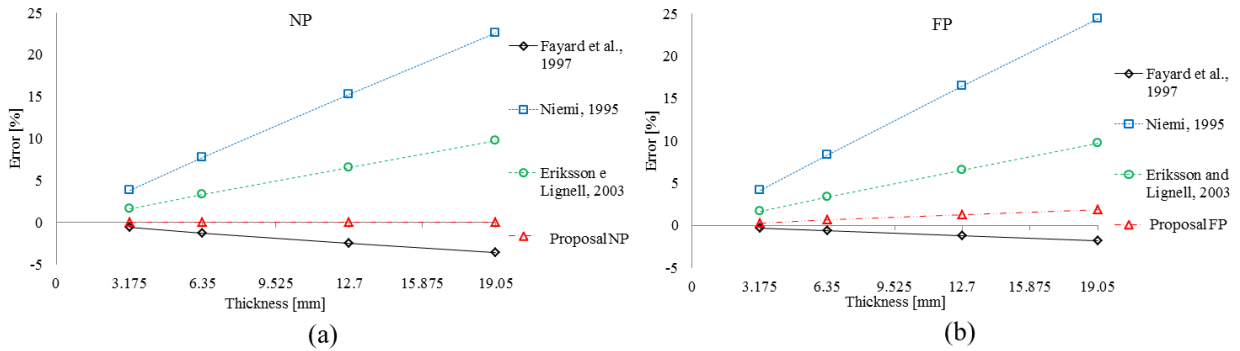


Figure 13. Mass error: (a) T-joint with weld fillets without penetration; (b) T-joint with full penetration weld fillets.

The error with respect to the first natural frequencies, Eq. (4), is presented in Fig. 14 for the component with weld fillets without penetration. Figure 15 presents the same results for the structure with full penetration weld fillets. In the Fig. 14, two different scales for the absolute error axis are presented in order to provide a better visualization for all results.

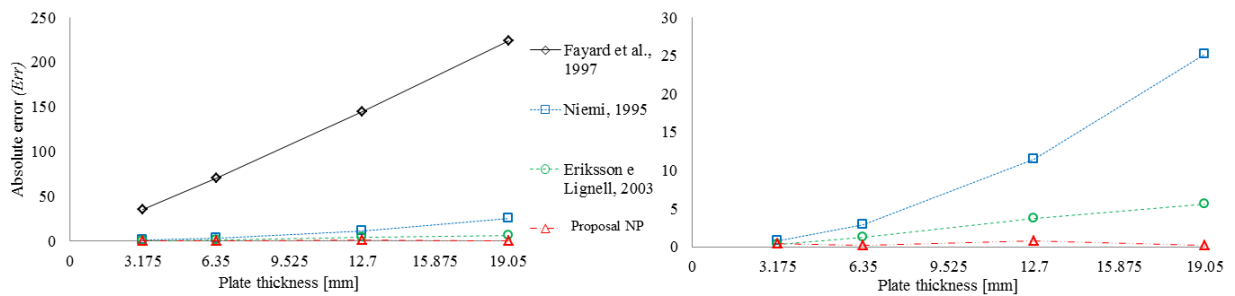


Figure 14. NP - Absolute error, Err .

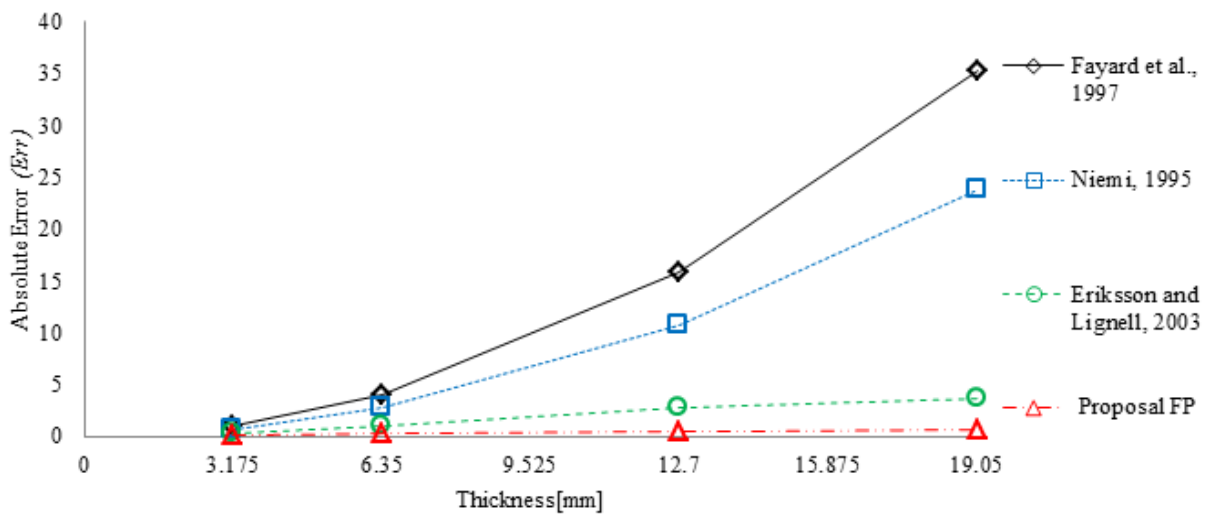


Figure 15. FP - Absolute error, Err .

As expected, both Proposal NP and FP presented the best results, minimizing the error with respect to the first natural frequencies. When representing the T-joint with weld fillets without penetration, the methodology of Fayard et al. (1997) presented a high error (10 times superior then the other methodologies), the performance of this methodology in the case of full penetration weld fillets was in agreement with the other two methodologies employed for comparison purposes.

It is important to stress that the minimization of an error function containing the natural frequencies is also implicitly preserving the stiffness of the structure. This is the main result of the present proposals, and seldom taken into account in other references.

5.3 Structural stress comparisson

The proposed methodologies were employed along the structural stress method in order to evaluate σ_{hs} . For comparison purposes, the same structures were also analyzed with well-established methodologies earlier presented. The geometry of study consists of a T-shaped welded structure with total dimensions equal to 254 mm X 260.35 mm X 508 mm ($w \times h + e \times p$). A plate thickness equal to 6.35 mm was considered.

The loading scenario consists of a pure tensile application. Both extremities of the horizontal plate, i.e., side edges, were clamped. A total force of 20KN was uniformly distributed by the top of the vertical plate. Figure 16 illustrates the loading scenario. The material was considered as a generic structural steel with Young's modulus equals 2.1×10^{11} MPa, Poisson's ratio equals 0.3 and mass density equals 7830 kg/m^3 .

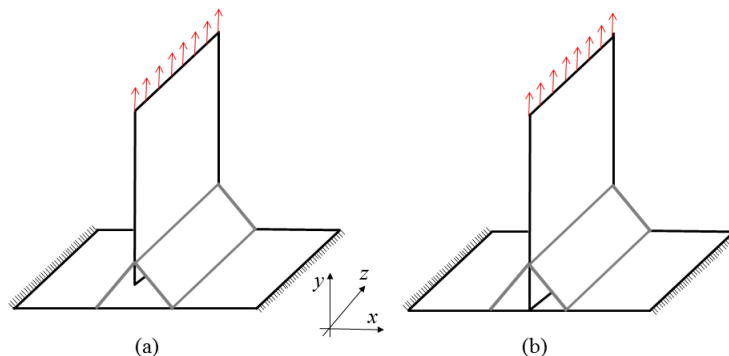


Figure 16. Loading scenario: (a) NP; (b) FP.

All methodologies were implemented with shell FE. The methodology proposed by Fayard (1997) was modeled using 4-node elements (SHELL181), and a mesh density in agreement with the size of the element E2. In this model, the rigid links were implemented with a multipoint constraint element (MPC184). All the other four methodologies employed 8-node high order shell elements (SHELL281) with fine mesh, i.e., element size equal to $0.4e$. The FE models, for comparison, were created according to the proposed by its respective authors. Table 2 presents the results for σ_{hs} and the difference between the results obtained by Proposals NP and FP with respect to the other three methodologies.

Table 2. Structural stress.

Structural Stress Methodology	Structural Stress		Difference Between Methodologies [%]	
	NP	FP	Proposal NP	Proposal FP
Fayard et al., 1997	81.52	83.41	-2.32	1.59
Niemi, 1995	88.58	88.59	5.83	7.35
Eriksson e Lignell, 2003	87.50	87.5	4.66	6.19
Proposal NP	83.42	-	-	-
Proposal FP	-	82.08	-	-

The agreement between results is clearly presented in Tab. 2. Both Proposals NP and FP obtained results for σ_{hs} , similar to the ones obtained by the methodologies employed for comparison. Once the structural stress is known, fatigue life could be easily evaluated employing S-N curves for the Fatigue Assessment Tool, FAT, of each analyzed geometry. As presented by Hobbacher et al. (2009), FAT 90 corresponds to the NP case, while FAT 100 corresponds to FP.

6. FINAL REMARKS

Both proposals were capable of accurately reproduce a T-joint welded component stiffness using shell FE. Proposals NP and FP successfully applied a virtual density aiming the mass conservation of the structure. Such feature can be highly desirable, especially in cases where the weld fillet comprises a significant amount of the structure total mass.

Proposal FP presented a minor error reproducing the mass of the structure, this can be explained by the fact that the virtual density is applied only to the mass of the weld fillet. However, in the case of fillets with full penetration, an additional area, and consequently mass, is necessary in order to produce a shell FE model. A different approach for inducing the mass conservation could be employed in order to circumvent this problem.

Both methodologies presented structural stresses in accordance with the results obtained by the other well established methodologies. These results ensure the consistency of the two proposals, nevertheless other tests with more complex geometries and loading scenarios are required in order to assess how robust these proposals are.

The major contribution of this work, in addition to the two proposals presented, is the methodology for obtaining optimum parameters for different welded structures. Using the same procedures employed in this work, one can formulate fitting rules for reproducing most of the structural details presented in the literature and standards.

7. ACKNOWLEDGEMENTS

The first author would like to acknowledge the financial support by the National Council for the Improvement of Higher Education (CAPES), and the second author acknowledges CNPq through grant 309685/2010-9.

8. REFERENCES

- ANSYS, R., 2012. *ANSYS Mechanical APDL*, Product Release 13.0 (2012). Ansys Inc., Canonsburg, Pennsylvania.
- Doerk, O.; Fricke, W.; Weissenborn, C. Comparison of different calculation methods for structural stresses at welded joints, *International journal of fatigue*, vol. 25(5), p. 359–369, 2003.
- Dong, P. A Structural Stress Definition and Numerical Implementation for Fatigue Analysis of Welded Joints, *International Journal of Fatigue*, vol. 23(10), p. 865–876, 2001.
- Eriksson, . and Lignell, A., 2003. *Weld Evaluation Using FEM: A Guide to Fatigue-loaded Structures*. Industrilitteratur.
- Fayard, J.-L., Bignonnet, A., and Van, K. D., 1997. Fatigue Design of Welded Thin Sheet Structures. *European Structural Integrity Society*, vol. 22, pp. 145152.
- Fermér, M., Andrasson, M., and Frodin, B., 1998. Fatigue Life Prediction of MAG-Welded Thin-Sheet Structures. *SAE Conference Proceedings*, pp. 4956. SOC Automotive Engineers INC.
- Fransson, P. and Pettersson, G. 2000. *Fatigue Life Prediction Using Forces in Welded Plates of Moderate Thickness*. PhD thesis, University of Karlskrona, Sweden.
- Fricke, W. et al., 2001. Recommended Hot Spot Analysis Procedure for Structural Details of FPSOs and Ships Based on Round-Robin FE Analyses. *11th International Offshore and Polar Engineering Conference*, vol. 4, pp. 8996.
- Fricke, W., 2003. Fatigue Analysis of Welded Joints: State of Development. *Marine Structures*, vol. 16, n. 3, pp. 185200.
- Hobbacher, A. et al., 2009. *Recommendations for Fatigue Design of Welded Joints and Components*. Welding Research Council, IIW.
- MATLAB. 2011. *The MathWorks Inc.*, version 7.12.0.635 (R2011a). Natick, Massachusetts.
- Matoba, M., Kawasaki, T., Fuji, T., and Yamauchi, T., 1983. Evaluation of Fatigue Strength of Welded Steel Structures-hulls Members, Hollow Section Joints, Piping and Vessel Joints. *IIW-Doc. -1082-83*. International Institute of Welding.
- Niemi, E., 1994. Recommendations Concerning Stress Determination for Fatigue Analysis of Welded Components. *IIW-Doc*. University of Technology.
- Niemi, E., 1995 *Stress Determination for Fatigue Analysis of Welded Components*. Woodhead Publishing.
- Niemi, E. and Tonskanen, P., 2000. IIS/IIW-1477-99 Hot Spot Stress Determination for Welded Edge Gussets. *Welding in the World -London-*, vol. 44, n. 5, pp. 3137.
- Radaj, D., 1990. *Design and Analysis of Fatigue Resistant Welded Structures*. Elsevier.
- van Wingerde, A. M., Packer, J. A., and Wardenier, J., 1995. Criteria for the Fatigue Assessment of Hollow Structural Section Connections, *Journal of Constructional Steel Research*, vol. 35, n. 1, pp. 71115.

9. RESPONSIBILITY NOTICE

The authors are the only responsible for the printed material included in this paper.